

## SPECTROSCOPY AND MASS MEASUREMENTS OF NEUTRON RICH ISOTOPES BY THE (t, $\alpha$ ) REACTION

E. R. Flynn, Ronald E. Brown, J. W. Sunier, D. G. Burke<sup>\*)</sup>, F. Ajzenberg-Selove<sup>†</sup>

J. A. Cizewski<sup>\*\*)</sup>

Los Alamos National Laboratory, Los Alamos, NM 87545 USA

### Abstract

The neutron excess of the triton makes it possible to use this projectile in transfer reactions to reach nuclei of greater neutron excess than the target nucleus. Principal examples of such reactions are the (t,  $\alpha$ ), (t, p) and (t,  $^3\text{He}$ ) reactions, all of which have been used to study neutron rich nuclei. The present report discusses several of these examples and reports on more definitive mass measurements and spectroscopy of the low lying levels of some of these nuclei. In particular, results of using a polarized triton beam are discussed as this study leads to many new spin assignments.

### 1. Introduction

The availability of a triton beam at the Los Alamos National Laboratory has allowed the reaction study of a large number of neutron rich nuclei over the recent years. There are three principal reactions which are used in this program. The two neutron transfer reaction (t, p), adds two neutrons to the target nucleus and this reaction on a neutron excess target yields results on nuclei beyond the neutron stability line. The proton pickup reaction (t,  $\alpha$ ), also increases the neutron excess since it reduces the proton number by one. Finally, the charge exchange reaction (t,  $^3\text{He}$ ) changes a proton into a neutron and again increases the neutron excess. All of these reactions produce not only a measure of the final mass value but also yield information regarding the low lying level energies, spin values, and spectroscopic values of various levels. In this regard, a polarized triton beam is capable of increasing the information obtained by measuring the analyzing power ( $A_y$ ). This latter feature is especially important in the case of the (t,  $\alpha$ ) reaction where large  $A_y$  values permit definitive spin assignments.

The studies discussed here are all part of a nuclear spectroscopy program aimed at a more thorough understanding of the complex interaction of elementary nuclear modes. In general, the studies have concentrated on regions of nuclear transitions, either transitions in nuclear shape or in coupling schemes. The use of the reactions discussed above permits an extension of the nuclear studies and their systematics to the more neutron rich regions which are difficult to reach by any other means. Thus an extensive investigation of the heavy rare earth region through the Ir and Au isotopes is a dominant part of this report as these represent a region where nuclei are going from deformed to spherical as the closed  $N = 126$  shell is approached. Another area discussed here is the nuclear region near  $A = 100$  where a complex interplay of collective and single particle effects produces rapid changes in nuclear shapes as well as subshell closure effects. The results of these studies yield a number of new mass measurements, a substantial number of new level assignments, and a large number of new spin assignments.

\*) McMaster University

†) University of Pennsylvania

\*\*\*) Yale University

### 2. Experimental Techniques

The work described here was carried out at the Los Alamos National Laboratory tandem Van de Graaff laboratory. All of the (t,  $\alpha$ ) and (t, p) data were taken using a 17 MeV beam while the (t,  $^3\text{He}$ ) data was obtained with a 22-25 MeV beam of tritons. The reaction products were detected in a Q3D spectrometer using a helix proportional counter in the focal plane<sup>1)</sup>. Typical energy resolutions of 12-20 keV were obtained, depending upon target thicknesses. Energy calibrations were performed for each isotope using targets with accurately known Q-values and excited state energies. Angular distributions were also measured and the results compared to distorted wave (DW) calculations in order to extract angular momentum transfers and spectroscopic values. In the case of polarized beam experiments, spin up and down measurements were obtained by flipping the direction of the triton spin<sup>2)</sup> at the source and repeating the run at each angle. These results were also compared to DW calculations as well as empirically to known spin states in nearby nuclei in order to extract the total spin transfer.

The targets were, in general, evaporated foils of thicknesses about 80 to 200 micrograms/cm<sup>2</sup>, depending upon the experiment. The Hg targets discussed below required special attention and consisted of a Hg compound deposited on a thin C backing.

### 3. Mass Measurements with the Triton Beam

Table 1 contains the results of a number of mass measurements made with various triton induced reactions over the last several years. There are 20 cases listed, 12 from the (t,  $\alpha$ ) reaction, 3 from the (t, p) reaction and 5 from the (t,  $^3\text{He}$ ) reaction. In all but the In cases, the assigned mass errors are 20 keV or less; the In results were done with thick targets because of the very low cross sections observed in this case. The masses of  $^{203}\text{Au}$ ,  $^{200}\text{Pt}$ , and  $^{82}\text{As}$  had not previously been measured and were only predicted by systematics. The nucleus  $^{243}\text{Np}$  had never been observed before and represents a new nuclide on the chart of the nuclides. Large disagreements exist with several previous mass measurements, especially with beta-decay results. Most notable among these are the masses of  $^{69}\text{Cu}$ ,  $^{103}\text{Tc}$ ,  $^{109}\text{Rh}$ ,  $^{159}\text{Eu}$ ,  $^{100}\text{Nb}$ , and  $^{124}\text{In}$ . The present measurement of  $^{69}\text{Cu}$  confirms the recent measurement of this mass by the (d,  $^3\text{He}$ ) reaction and places the beta-decay results in error. The  $^{103}\text{Tc}$  and  $^{109}\text{Rh}$  results, which are discussed further below, considerably exceed the errors assigned to them in Ref. 17. It is interesting that a large part of the error that the present work must assign to the  $^{109}\text{Rh}$  mass comes from the uncertainty in the mass of the target nucleus,  $^{110}\text{Pd}$ , a stable nucleus. The large error in the mass of  $^{100}\text{Nb}$  between the current results and that reported in Ref. 17 is still a subject of controversy as a recent beta-decay measurement [19] confirms the older result. A close check of the  $^{100}\text{Mo}(t, ^3\text{He})$  data still precludes the beta-decay result and there is no reason to change the reaction data result.

Table 1  
Recent Mass Measurements Made with the Triton Beam

Nucleus	Reaction	Q(keV)	Ref.	Mass Excess		Error (keV)
				Present (keV)	Published (keV)	
$^{69}\text{Cu}$	$^{70}\text{Zn}(t, \alpha)$	$8682 \pm 20$	3	$-65717 \pm 21$	$-65940 \pm 70^{(b)}$	-223
$^{103}\text{Tc}$	$^{104}\text{Ru}(t, \alpha)$	$9048 \pm 20$	4	$-84622 \pm 30$	$-84910 \pm 100$	-288
$^{109}\text{Rh}$	$^{110}\text{Pb}(t, \alpha)$	$8993 \pm 20$	4	$-84805 \pm 40$	$-85110 \pm 100$	-305
$^{153}\text{Pm}$	$^{154}\text{Sm}(t, \alpha)$	$10748 \pm 20$	5	$-70676 \pm 20$	$-70760 \pm 100^{(c)}$	-84
$^{157}\text{Eu}$	$^{158}\text{Gd}(t, \alpha)$	$11302 \pm 6$	6	$-69469 \pm 8$	$-69465 \pm 16$	+5
$^{159}\text{Eu}$	$^{160}\text{Gd}(t, \alpha)$	$10636 \pm 8$	6	$-66054 \pm 10$	$-65930 \pm 50$	+151
$^{185}\text{Ta}$	$^{186}\text{W}(t, \alpha)$	$11430 \pm 20$	7	$-41403 \pm 22$	$-41360 \pm 21$	+43
$^{195}\text{Ir}$	$^{196}\text{Pt}(t, \alpha)$	$11545 \pm 20$	8	$-31672 \pm 20$	$-31692 \pm 31$	+20
$^{197}\text{Ir}$	$^{198}\text{Pt}(t, \alpha)$	$10885 \pm 20$	8	$-28281 \pm 30$	$-28430 \pm 200$	+149
$^{201}\text{Au}$	$^{202}\text{Hg}(t, \alpha)$	$11567 \pm 15$	9	$-26389 \pm 15$	$-26400 \pm 100$	-11
$^{203}\text{Au}$	$^{204}\text{Hg}(t, \alpha)$	$10962 \pm 15$	9	$-23131 \pm 15$	$(-22980)^{(d)}$	(+151)
$^{243}\text{Np}$	$^{244}\text{Pu}(t, \alpha)$	$12405 \pm 10$	10	$-59923 \pm 10$	-- <sup>(e)</sup>	---
$^{200}\text{Pt}$	$^{198}\text{Pt}(t, p)$	$4356 \pm 20$	11	$-26616 \pm 20$	$(26600)^{(d)}$	(+16)
$^{246}\text{Pu}$	$^{244}\text{Pu}(t, p)$	$2085 \pm 20$	12	$-65380 \pm 20$	$-65290 \pm 50$	+90
$^{78}\text{Ge}$	$^{76}\text{Ge}(t, p)$	$6310 \pm 8$	13	$-71862 \pm 8$	$-71760 \pm 70$	+102
$^{82}\text{As}$	$^{82}\text{Se}(t, ^3\text{He})$	$-7500 \pm 25$	14	$-70067 \pm 27$	$(-70190)^{(d)}$	(-123)
$^{80}\text{As}$	$^{80}\text{Se}(t, ^3\text{He})$	$-5560 \pm 25$	14	$-72182 \pm 27$	$-72060 \pm 300$	+122
$^{100}\text{Nb}$	$^{100}\text{Mo}(t, ^3\text{He})$	$-6690 \pm 30$	15	$-79480 \pm 30$	$-79960 \pm 130^{(f)}$	-480
$^{122}\text{In}$	$^{122}\text{Sn}(t, ^3\text{He})$	$-6350 \pm 50$	16	$-83580 \pm 50$	$-83600 \pm 150$	-20
$^{124}\text{In}$	$^{124}\text{Sn}(t, ^3\text{He})$	$-7590 \pm 50$	16	$-80630 \pm 50$	$-81100 \pm 90$	-470

- (a) Reference 17.  
(b)  $(d, ^3\text{He}) + -65750 \pm 10$   
(c)  $(d, ^3\text{He}) + -70622 \pm 15$ , Ref. 18.  
(d) Systematic value only.  
(e) Not previously observed.  
(f)  $\beta$ -decay  $+ -79949 \pm 100$ , Ref. 19.

All of the present results were obtained by observation of the states at several angles and averaging the energies. As stated above, separate calibration targets were used and a constant energy calibration of the Q3D spectrometer was not assumed. It is, of course, possible that a ground state is not populated in a specific reaction but in all the cases quoted here, this was considered to be an unlikely possibility. The exception is for  $^{243}\text{Np}$  where there were no nearby systematics with compare to and many very weak states exist in the spectrum. Here one can only make the statement that no states exist with higher alpha energies than observed and the mass reported is most likely the ground state.

#### 4. Neutron Rich Ir and Au Isotopes

We have obtained recent results on the neutron rich isotopes of Ir and Au through the use of the  $(t, \alpha)$  reaction. This study was done with a polarized triton beam and the  $A_y$  values were then used to obtain spin values for the single particle proton states. A spectrum for the  $^{198}\text{Pt}(t, \alpha)^{197}\text{Ir}$  reaction, the most neutron rich Pt target available, is shown in Fig. 1. The results are from Ref. 20 and the ground state mass of  $^{197}\text{Ir}$  is given in Table 1. A similar spectrum for the  $^{204}\text{Hg}(t, \alpha)^{203}\text{Au}$  reaction is shown in Fig. 2. Examples of differential cross sections and  $A_y$  values are shown in Figs. 3 and 4 for these two cases, respectively. The solid lines in these

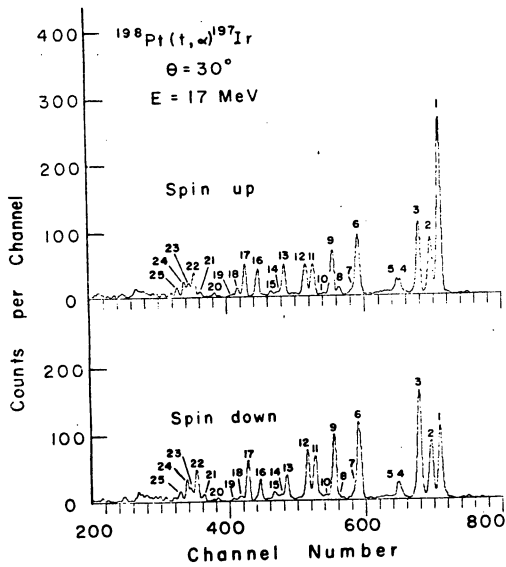


Fig. 1.  $^{198}\text{Pt}(t, \alpha)^{197}\text{Ir}$  spectra.

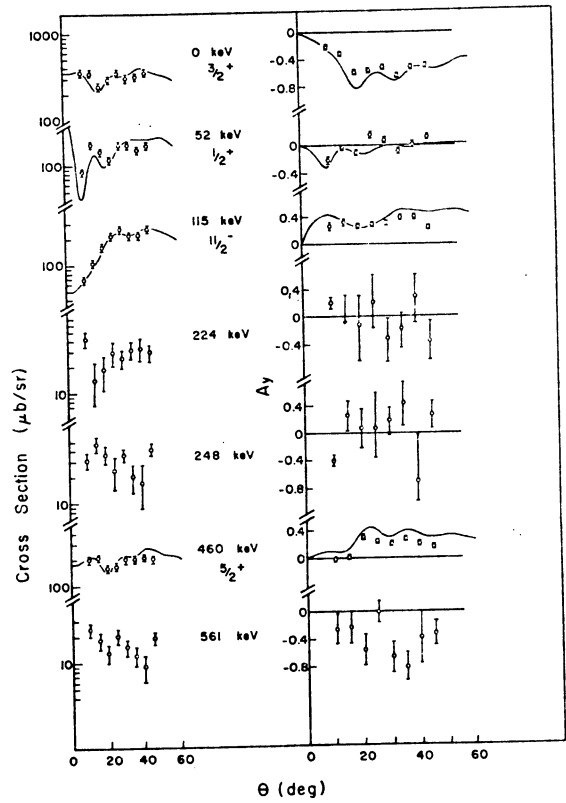


Fig. 3. Examples of  $d\sigma/d\Omega$  and  $A_y$  for the  $^{198}\text{Pt}(t, \alpha)^{197}\text{Ir}$  reaction.

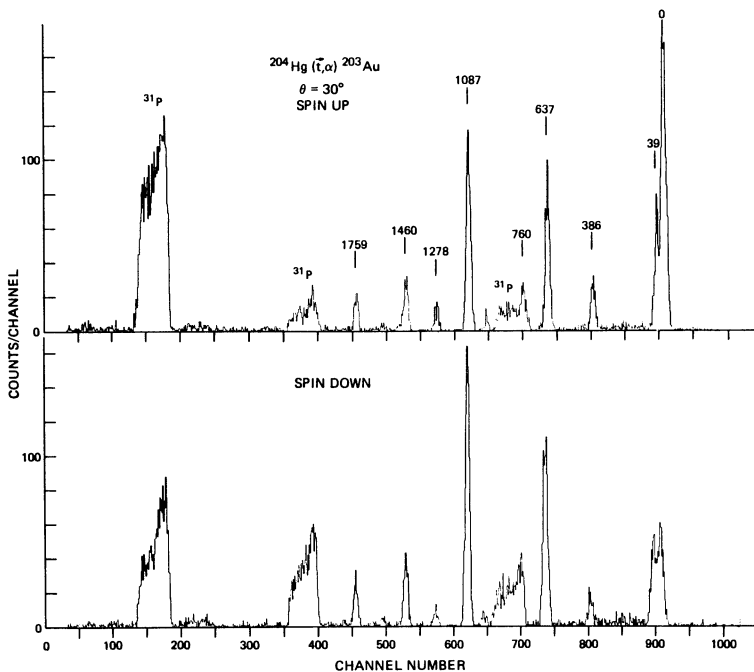


Fig. 2.  $^{204}\text{Hg}(t, \alpha)^{203}\text{Au}$  spectrum.

figures are DW calculations. Table 2 contain the results of this analysis for  $^{195,197}\text{r}$  and  $^{201,203}\text{Au}$ . The table contains the excitation energies, spin values and relative spectroscopic strengths, the latter being relative to  $^{207}\text{Tl}$  which is presumably a rather pure shell model nucleus.

The results of Table 2 indicate the value of reaching these neutron excess nuclei off the stability line. The rapidly increasing complexity in the spectrum is easily seen from this table which presents the low lying levels up to about 1.5 MeV (in the case of  $^{203}\text{Au}$ , the levels shown are the only observed ones up to 2.5 MeV). Although there is some fragmentation of the levels in  $^{203}\text{Au}$  over the single state per orbital of  $^{207}\text{Tl}$ , the spectrum is still relatively simple and all the  $h_{11/2}$  and  $d_{5/2}$  strength is basically seen with the reduced  $d_{3/2}$  and  $s_{1/2}$  strength reflecting the removal of two more protons relative to Tl. In going to  $^{201}\text{Au}$ , there is already a dramatic trend towards more collective phenomena with an increased fractionization of levels and a reduction in overall spectroscopic strength. Thus the trend towards the very collective condition which produces deformation in the nearby rare earths and, indeed in the lighter Hg nuclei [21], is already evidenced this close to the closed shell. In this case  $^{203}\text{Hg}$  serves to indicate the total unperturbed single hole proton strength expected here as well as the energy centroids of the strength before the collective force becomes important.

Table 2

Results of ( $\vec{t}, \alpha$ ) Reaction on the Hg and Pt Isotopes											
$^{203}\text{Au}$			$^{201}\text{Au}$			$^{197}\text{Ir}$			$^{195}\text{Ir}$		
$E_x$ (keV)	$J^\pi$	$S_{\text{rel}}$	$E_x$ (keV)	$J^\pi$	$S_{\text{rel}}$	$E_x$ (keV)	$J^\pi$	$S_{\text{rel}}$	$E_x$ (keV)	$J^\pi$	$S_{\text{rel}}$
0	$3/2^+$	0.62	0	$3/2^+$	0.44	0	$3/2^+$	0.43	0	$3/2^+$	0.26
39	$1/2^+$	0.44	101	$1/2^+$	0.23	52	$1/2^+$	0.35	69	$1/2^+$	0.22
386	$3/2^+$	0.10	359	$3/2^+$	0.05	115	$11/2^-$	0.58	100	$11/2^-$	0.36
637	$11/2^-$	0.61	594	$11/2^-$	0.44	224			176	$5/2^+$	0.02
760	$5/2^+$	0.10	653	$5/2^+$	0.27	248			235	$(3/2)^+$	0.04
851			810	$5/2^+$	0.03	460	$5/2^+$	0.32	288	$3/2^+$	0.06
1087	$5/2^+$	0.65	897	$1/2^+$	0.09	495			397		
1278	$1/2^+$	0.06	1055	$3/2^+$	0.07	561			415		
1460	$11/2^-$	0.21	1216	$5/2^+$	0.12	606	$5/2^+$	0.25	503	$5/2^+$	0.27
1759	$(5/2^+)$	(0.12)	1242	$(5/2^+)$	0.07	654			542	$3/2^+$	0.03
			1465	$5/2^+$	0.20	715	$11/2^-$	0.26	584	$5/2^+$	0.14
			1506	$11/2^-$	0.21	761	$5/2^+$	0.16	628		
						885			721	$11/2^-$	0.27
						924			764	$5/2^+$	0.10
						960			879	$5/2^+$	0.05
									911		
						1043	$1/2^+$	0.11	958		
						1116	$11/2^-$	0.26			
						1160			995	$11/2^-$	0.16
						1202			1019	$1/2^+$	0.22
						1300			1052	$11/2^-$	0.15
						1384	$(5/2^+)$	0.03	1109		
						1426	$(5/2^+)$	0.12	1170	$3/2^+$	0.04
						1459			1233		
						1485	$(5/2^+)$	0.08	1369		

The removal of two more protons and neutrons from the Au case again considerably increases the complexity as seen in Table 2. Here the Ir isotopes now have a large number of levels below 1.5 MeV and are much more reminiscent of the deformed nuclei (see, for example, Ref. 7). Again a comparison of the two most neutron rich cases considered here show the reduction of strength as one goes away from the closed  $N = 126$  shell with  $^{195}\text{Ir}$  containing less total relative strength than  $^{197}\text{Ir}$  where the sum of the  $h_{11/2}$  and  $d_{5/2}$  relative strength equals approximately one as in the  $^{203}\text{Au}$  results. Another very interesting point to make here is the rapid descent of the  $h_{11/2}$  strength in excitation energy in going from  $^{203}\text{Au}$  to  $^{195}\text{Ir}$ . This orbital is usually associated with deformation and its lowering in the spectrum is a sign of the onset of a shape deformation. Thus by examining these heaviest isotopes we are able to more clearly see the trend away from a simple shell model picture towards a collective deformed picture.

##### 5. Neutron Rich Nuclei Near $A = 100$

The polarized ( $\vec{t}, \alpha$ ) reaction has also been extensively employed near  $A = 100$  to study the complex interplay of collective and single particle interactions which takes place in this region. Here it is known from fission fragment studies [22] that a shape transition occurs in the neutron rich isotopes near  $A = 100$  while at  $N = 56$  there is a subshell closure [23] in certain nuclei. Coincident with these phenomena, a strong isospin interaction occurs between the  $g_{7/2}$  neutron and the  $g_{9/2}$  proton states which is thought to be responsible for the deformation onset [24]. However, when sufficient particles are present this tendency is overcome by the pairing correlations and a spherical trend is resumed. Thus a knowledge of the proton strength of the most neutron rich isotopes as well as the systematic behavior of this strength as a function of neutron number for several elements is important to test these concepts. Figure 5 contains a spectrum of the

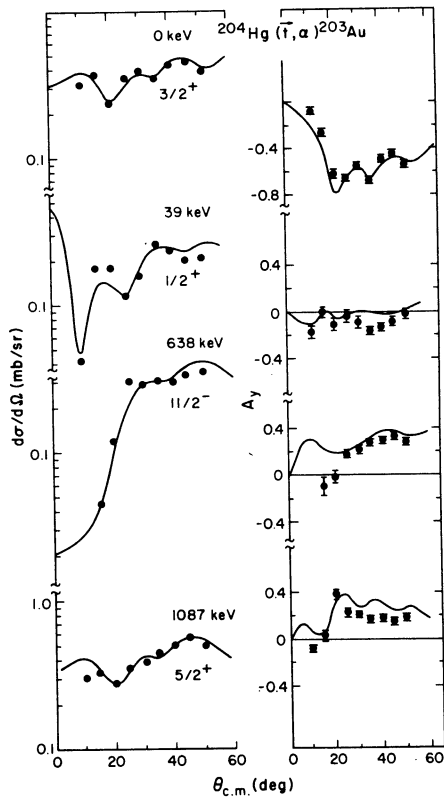


Fig. 4. Examples of  $d\sigma/d\Omega$  and  $A_y$  for the  $^{204}\text{Hg}(t, \alpha)^{203}\text{Au}$  reaction.

$^{110}\text{Pd}(t, \alpha)$  reaction; the nucleus  $^{109}\text{Rh}$  had no known levels before this experiment [4]. Examples of differential cross sections and  $A_y$  values with DW calculations are shown in Fig. 6. A similar experiment was also carried out on  $^{104}\text{Ru}$  leading to the first level scheme for  $^{103}\text{Tc}$  [4]. It is interesting to examine the systematics of the neutron rich elements in this region in light of these new data. Figure 7 contains the level schemes for the low-lying levels of  $^{95}\text{Y}$ ,  $^{95}\text{Nb}$ ,  $^{103}\text{Tc}$ , and  $^{109}\text{Rd}$  from Refs. [4,25]. The subshell closure at  $Z = 40$  is obvious from this figure which clearly shows the large drop in energy of the  $g_{9/2}$  orbital relative to the  $p_{1/2}$  in going from  $^{95}\text{Y}$  to  $^{95}\text{Nb}$  ( $Z = 39$  to  $Z = 41$ ). However, another dramatic effect occurs at  $Z = 43$ , in  $^{103}\text{Tc}$ , where a substantial rearrangement of orbitals takes place with the  $3/2^-$  and  $5/2^-$  dropping below the  $9/2^+$  and  $1/2^-$ . This trend is reversed again in  $^{109}\text{Rd}$  where the normal ordering for this region is resumed. As a further illustration of the unusual behavior of  $^{103}\text{Tc}$ , the single hole states shown in this figure do not contain the ground state but rather, the ground and first excited states have spins  $5/2^+$  and  $7/2^+$ , respectively; these states have only weak single hole proton strength and belong in the next shell. Indeed, the arrangement of spin states as shown in the systematics of the Tc isotopes in Fig. 8, is reminiscent of a deformed nucleus with bands being based on the  $5/2^+$  and the  $3/2^-$  states. Such bands might be based on the Nilsson orbitals  $5/2^+ [422]$  arising from the  $g_{9/2}$  orbital and  $3/2^- [302]$  arising from the  $p_{3/2}$  orbital. A transitional character is still suggested for this nucleus as the bands do not have the same band energy.

We are currently studying the systematics of the Nb-Tc-Rh isotopes through the  $(t, \alpha)$  reaction in order to plot out the region of transition which seems to occur in the neutron rich isotopes. In Fig. 9 we show the results for  $^{95}\text{Y}$ ,  $^{97}\text{Y}$ ,  $^{99}\text{Nb}$  to illustrate how the trends of the single hole strength proceed with neutron number here. There is considerable contrast here with the Tc results illustrated above. First of all,  $^{97}\text{Nb}$  shows a large effect due to the  $N = 56$  subshell closure in that the

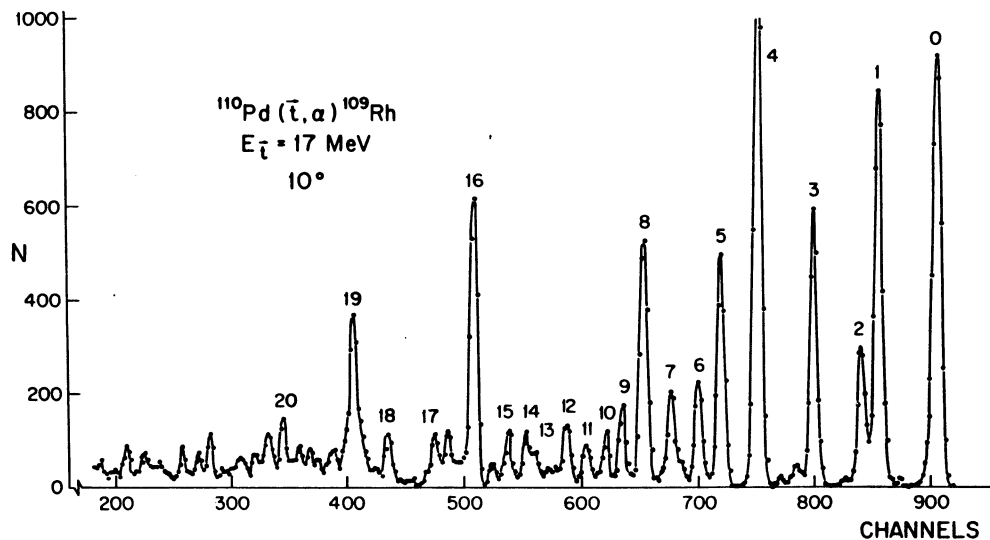


Fig. 5.  $^{110}\text{Pd}(t, \alpha)^{109}\text{Rh}$  spectrum.

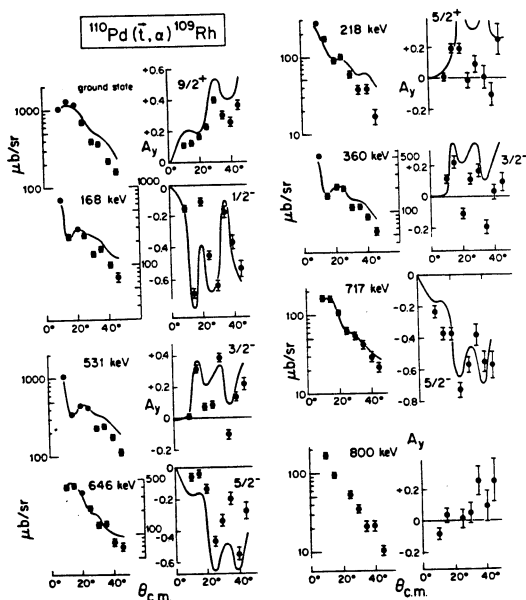


Fig. 6. Examples of  $d\sigma/d\Omega$  and  $A_y$  for the  $^{110}\text{Pd}(t,\alpha)^{109}\text{Rh}$  reaction.

level spacing is increased with a resulting simpler level structure at low excitation.  $^{99}\text{Nb}$  does not show this feature although it also contains 56 neutrons, but rather shows a gradual increase in the energy of the  $1/2^-$  state and a decreasing energy for  $3/2^-$ ,  $5/2^+$  and  $7/2^+$  states which follows the trend of the other isotopes. A recent (t,p) study of the Mo isotopes also indicated no evidence for the  $N = 56$  subshell closure which thus seems to disappear above  $Z = 41$ .

Experiments on the Rh isotopes are also under way to complete this mapping of the deformation region near  $A = 100$ . The current results indicate the complexity of the phenomena with significant effects due to the addition of only one or two particles. This region represents a severe challenge to theoretical approaches because of this complex behavior and models such as the IBA [26] must introduce additional degrees of freedom in order to reproduce even the qualitative trends of one chain of isotopes.

#### 6. The $^{198}\text{Pt}(t,p)^{200}\text{Pt}$ experiment

As an illustration of the success of the (t,p) reaction in the study of neutron rich nuclei, Table 3 contains the results of an experiment  $^{198}\text{Pt}(t,p)^{200}\text{Pt}$ , using a beam of 17 MeV tritons. This is the first data obtained on the level scheme for  $^{200}\text{Pt}$  and the table illustrates the extensive data obtainable by this technique. In this experiment [11] the goal was to examine the symmetries predicted by the IBA model in the transition region represented by the heavy rare earths through lead. The results showed clearly the trend towards a vibrational character of  $^{200}\text{Pt}$  over the lighter Pt isotopes which have a gamma unstable shape. Of particular importance, these new data extend the test of the IBA model into the neutron rich area where the trend towards vibrational or SU(3) symmetry exists. Comparison of the model predictions to the energy positions of excited  $0^+$  and  $2^+$  states and also with (t,p) ground state cross sections yields a relatively smooth variation of the IBA parameters. Another interesting feature

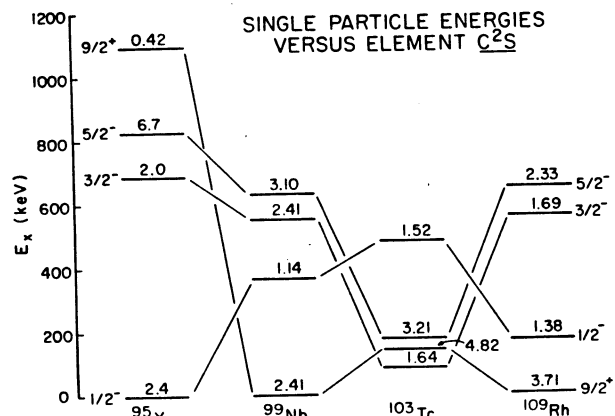


Fig. 7. Systematics of proton hole states for  $^{95}\text{Y}$ ,  $^{99}\text{Nb}$ ,  $^{103}\text{Rh}$  and  $^{109}\text{Rh}$ .

of this experiment was the lack of observation of a pairing vibration state (a search in excitation energy much higher than shown in the table was made for such a  $0^+$  state and not seen). This nonobservation indicates the small overlap that exists between the  $^{198}\text{Pt}$  transitional ground state and the spherical pairing vibration state.

#### 7. Future trends and summary

The techniques described here using a triton beam to study neutron rich nuclei have achieved appreciable success in both the increased accuracy of mass measurements and in the new spectroscopy of these nuclides. In addition to the distinct attributes of a triton beam, the power of the experimental program discussed above lies in the use of a large solid angle spectrometer, a Q3D, and a variety of focal plane detectors for this instrument. These detectors have been designed to not only yield excellent energy resolution but also particle selection and background rejection [27]. This system is thus amenable to more difficult experiments than those discussed here and which involve either other types of beams, very low cross section reactions or special targets.

The first two of this type of experiments have been in progress recently at Los Alamos using a  $^{14}\text{C}$  beam [28,29]. The principle reactions used by the group conducting these experiments are the  $(^{14}\text{C},^{16}\text{O})$  and  $(^{14}\text{C},^{14}\text{O})$  reactions. The first of these, a two proton pickup reaction, obviously reaches a number of interesting neutron rich nuclei in a manner similar to the (t,α) reaction discussed above. The second reaction, a double charge exchange reaction, is rather exotic but potentially very interesting as it appears to be the only promising way to reach certain exciting nuclei e.g.  $^{100}\text{Mo}(^{14}\text{C},^{14}\text{O})^{100}\text{Zr}$ . The cross sections for this reaction although small, are larger than expected [28] and much larger than the competing reaction  $(\pi, \pi^+)$ . These two reactions offer an exciting future to the study of neutron rich nuclei and the experimental techniques discussed above are directly applicable to this program.

Table 3. Results of  $^{198}\text{Pt}(\vec{t},p)$  Reaction

$E_x$ (keV)	$d\sigma/d\Omega$ ( $\mu\text{b}/\text{sr}$ ) ( $25^\circ$ )	L	$J^\pi$
0	342(14)	0	$0^+$
466(6)	6.7(11)		$(2^+)$
863(6)	3.5(7)	(2)	$(2^+)$
1099(6)	16.8(13)	(4)	$(4^+)$
1263(5)	24(2)	(4)	$(4^+)$
1561(7)	2.2(8)		
1579(6)	5.1(8)	0	$0^+$
1617(8)	1.6(8)		
1684(9)	1.5(8)		
1726(6)	5.3(11)	(2)	$(2^+)$
1757(5)	7.9(12)	(2)	$(2^+)$
1842(7)	3.7(9)	(2)	$(2^+)$
1872(5)	3.9(9)		
1915(5)	4.2(9)		
1936(5)	13.9(15)	(4)	$(4^+)$
1986(5)	6.3(10)	(2)	$(2^+)$
2014(6)	7.8(15)	0	$0^+$
2118(7)	6.4(10)	(2)	$(2^+)$
2128(7)	5.9(12)		
2144(6)	2.4(17)		
2156(6)	13(2)	(2)	$(2^+)$
2168(6)	6.0(10)		
2253(7)	6.7(10)	0	$0^+$
2299(7)	3.2(8)		
2402(9)	3.3(8)		
2431(7)	4.7(9)		
2461(8)	3.8(11)	(4)	$(4^+)$
2491(10)	0.8(7)		
2525(10)	1.9(8)		
2551(8)	7.1(13)		
2668(9)	17(2)	(2)	$(2^+)$
2709(9)	3.8(9)		
2731(11)	2.7(9)		

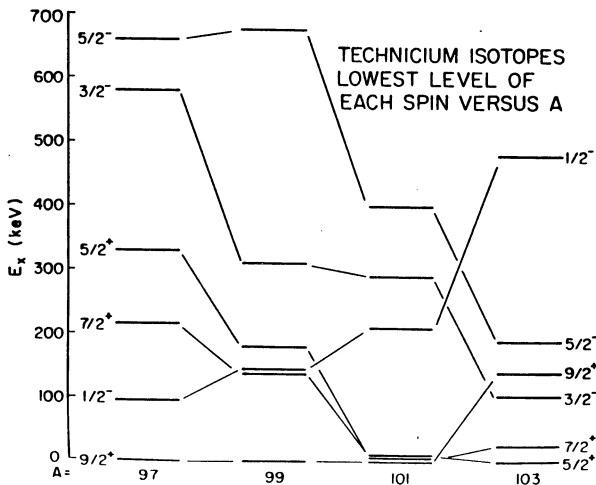


Fig. 8. Systematics of low-lying states in the Tc isotopes.

SYSTEMATICS OF LOW LYING LEVELS IN Nb ISOTOPES

NUMBERS ABOVE LINES ARE ( $\vec{t}, \alpha$ ) SPECTROSCOPIC FACTORS

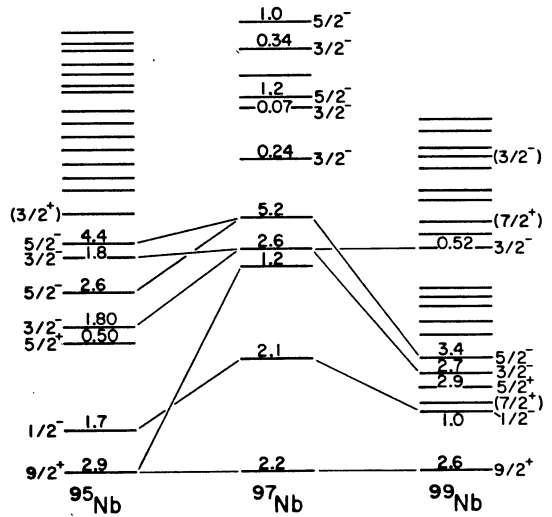


Fig. 9. Systematics of low-lying states in the Nb isotopes.

The third new program mentioned above involves the use of exotic targets and is discussed in more detail in a paper by J. Wilhelmy elsewhere in this conference [30]. Again one of the principal assets we have in such a new program is the extreme sensitivity of the spectrometer and detector system as well as the specialized beams such as the triton (polarized and unpolarized), and  $^{14}\text{C}$  beams. As far as neutron rich nuclei which could be studied with the use of exotic targets, the outstanding examples are found from the targets  $^{32}\text{Si}$  and  $^{60}\text{Fe}$ . These targets which are obtainable from the LAMPF beam stop, as discussed in Ref. 30, may be quite thin as experiments with as little as 10-15  $\mu\text{g}/\text{cm}^2$  have been carried out. However, the available materials from the LAMPF irradiations should, in general, permit much thicker targets than that. Planned experiments on the  $^{32}\text{Si}$  target are the (t,p) reaction which will reach the  $N = 20$  closed shell at  $^{34}\text{Si}$ , and the (t, $\alpha$ ) reaction which will measure the spectroscopy of  $^{31}\text{Al}$  for the first time. Similar studies will be made on  $^{60}\text{Fe}$  with the (t,p) reaction reaching to  $^{62}\text{Fe}$ , the (t, $^3\text{He}$ ) reaction to the unobserved nucleus  $^{60}\text{Mn}$ , and the (t, $\alpha$ ) reaction to  $^{59}\text{Mn}$ , again a nucleus with unknown spectroscopy. In addition to the general nuclear physics interest in these nuclei off the stability line, there is special astrophysics interest in these nuclei especially in the Fe region because of the nucleosynthesis problems [31]. These and many other exotic targets with half-lives sufficiently long, promise to make this an exciting field for some time to come.

### References

1. E. R. Flynn, S. Orbesen, J. D. Sherman, J. W. Sunier and R. Woods, Nucl. Instr. Methods, 128, 35 (1975).
2. R. A. Hardekopf, Proc. of the 4th Int. Sym. on Pol. Phenomena in Nucl. Reactions, 1975, edited by W. Gruebler, p. 865.
3. F. Ajzenberg-Selove, R. E. Brown, E. R. Flynn and J. W. Sunier (to be published).
4. E. R. Flynn, F. Ajzenberg-Selove, R. E. Brown, J. A. Cizewski and J. W. Sunier, Phys. Rev. C. (to be published).
5. D. G. Burke, E. R. Flynn and J. W. Sunier, Phys. Rev. C18 (1978) 693.
6. D. G. Burke, G. Lozhóiden, E. R. Flynn and J. W. Sunier, Nucl. Phys., A318 (1979) 77.
7. G. Lozhóiden, D. G. Burke, E. R. Flynn and J. W. Sunier, Physca. Scripta. 22 (1980) 203.
8. J. A. Cizewski, D. G. Burke, E. R. Flynn, R. E. Brown and J. W. Sunier, Phys. Rev. Letts. (to be published).
9. E. R. Flynn, D. G. Burke, R. E. Brown, J. A. Cizewski, and J. W. Sunier (to be published).
10. E. R. Flynn, D. L. Hanson and R. A. Hardekopf, Phys. Rev. C19 (1979) 355.
11. J. A. Cizewski, E. R. Flynn, R. E. Brown, D. L. Hanson, S. D. Orbesen and J. W. Sunier, Phys. Rev. C23 (1981) 1453.
12. R. E. Brown, J. A. Cizewski, E. R. Flynn and J. W. Sunier, Phys. Rev. C20 (1979) 1301.
13. D. Ardouin, C. Lebrun, F. Guilbault, B. Remaud, E. R. Flynn, D. L. Hanson, S. D. Orbesen, M. N. Vergnes, G. Rotbard and K. Kumar, Phys. Rev. C18 (1978) 1201.
14. F. Ajzenberg-Selove, E. R. Flynn, D. L. Hanson and S. D. Orbesen, Phys. Rev. C19 (1979) 1742.
15. F. Ajzenberg-Selove, E. R. Flynn, D. L. Hanson and S. Orbesen, Phys. Rev. C19 (1979) 2068.
16. F. Ajzenberg-Selove, E. R. Flynn, J. W. Sunier and D. L. Hanson, Phys. Rev. C17 (1978) 960.
17. A. H. Wapstra and K. Bos, At. Nucl. Data Tables 19 (1977) 177.
18. B. Zeidman and J. A. Nolen, Phys. Rev. C18 (1978) 2122.
19. R. Stipler et al., Z. Phys. A284 (1978) 95.
20. J. A. Cizewski, D. G. Burke, E. R. Flynn, R. E. Brown and J. W. Sunier (to be published).
21. C. M. Lederer, V. S. Shirley, Table of Isotopes, 7th edition (John Wiley & Sons 1978).
22. K. Sistemich, W. D. Lauppe, H. Lawin, H. Seyforth and B. D. Kern, Z. Physik A289, (1979) 225.
23. E. R. Flynn, J. G. Beery and A. G. Blair, Nucl. Phys. A218 (1974) 285.
24. P. Federman and S. P. Pittel, Phys. Rev. C20 (1979) 820.
25. E. R. Flynn, R. E. Brown, and F. Ajzenberg-Selove (to be published).
26. A. Arima and F. Iachello, Phys. Rev. Lett. 35 (1975) 1069.
27. E. R. Flynn, Nucl. Inst. Methods 162 (1979) 305.
28. J. C. Peng, N. Stein, J. W. Sunier, D. M. Drake, J. D. Moses, J. A. Cizewski and J. R. Tesmer, Phys. Rev. Letts. 43 (1979) 675.
29. D. M. Drake, J. D. Moses, J. C. Peng, N. Stein and J. W. Sunier, Phys. Rev. Letts. 45 (1980) 1765.
30. J.B. Wilhelmy, G. E. Bentley, K. E. Thomas, R. E. Brown, E. R. Flynn, J. van der Plicht, L. G. Mann and G. L. Stuble, Proceedings of this conference.
31. G. M. Fuller, W. A. Fowler and M. J. Newman, The Astrophysical Journal Supp. Sers. 42 (1980) 447.